Josephson effect in a fractal geometry

Morten Amundsen,[1] Vladimir Juričić,[2,3] and Jabir Ali Ouassou[4]
[1)] *Center for Quantum Spintronics, Department of Physics, Norwegian University of Science and Technology, NO-7491 Trondheim, Norway*
[2)] *Departamento de Física, Universidad Técnica Federico Santa María, Casilla 110, Valparaíso, Chile*
[3)] *Nordita, KTH Royal Institute of Technology and Stockholm University, Hannes Alfvéns väg 12, SE-106 91 Stockholm, Sweden*
[4)] *Department of Computer Science, Electrical Engineering and Mathematical Sciences, Western Norway University of Applied Sciences, NO-5528 Haugesund, Norway*

(Dated: 3 April 2024)

The Josephson effect is a hallmark signature of the superconducting state, which, however, has been sparsely explored in non-crystalline superconducting materials. Motivated by this, we consider a Josephson junction consisting of two superconductors with a fractal metallic interlayer, which is patterned as a *Sierpiński carpet* by removing atomic sites in a self-similar and scale-invariant manner. We here show that the fractal geometry has direct observable consequences on the Josephson effect. In particular, we demonstrate that the form of the supercurrent-magnetic field relation as the fractal generation number increases can be directly related to the self-similar fractal geometry of the normal metallic layer. Furthermore, the maxima of the corresponding diffraction pattern directly encode the self-repeating fractal structure in the course of fractal generation, implying that the corresponding magnetic length directly probes the shortest length scale in the given fractal generation. Our results should motivate future experimental efforts to verify these predictions in designer quantum materials.

Fractals are paradigmatic non-crystalline structures featuring a non-integer spatial dimension with a self-similarly repeating pattern at smaller and smaller length scales, which are rather ubiquitous in Nature, from living organisms to geological objects.[1] In the quantum realm, they are realized most commonly in terms of wavefunctions exhibiting a fractal behavior when electrons confined on a plane are subjected to a perpendicular magnetic field, e.g. in the Hofstadter butterfly[2], as well as in disordered electronic systems.[3,4] The interplay of fractal geometry in non-integer dimensions and quantum-mechanical collective behavior of electrons living on fractals has attracted renewed interest with advances in assembling of fractal structures[5] and the experimental observation of the emerging fractal features of the electronic wavefunctions.[6] These observations spurred further interest in this problem, especially in light of possible nontrivial topological properties of the electronic wavefunctions on the fractals.[7–16] Quite surprisingly, however, superconductivity in this context has been rather sparsely explored.[17–21] Intriguingly, a very recent study has however suggested that artificial fractal geometries can enhance the critical temperature T_c of superconductors.[18]

Superconductivity is a macroscopic quantum phenomenon, where a large number of electron pairs all condense into the same macroscopic quantum state. This quantum state can be described using a macroscopic wave function $\Psi(\boldsymbol{r},t) = |\Psi(\boldsymbol{r},t)|e^{i\varphi(\boldsymbol{r},t)}$. When two different superconductors are connected to the same metal, their wave functions can leak into the metal and interfere with each other. This can result in the *Josephson effect*,[22,23] whereby a current that depends on the phase difference $\delta\varphi$ between the wavefunctions in the two superconductors flows through the normal metal. Josephson junctions have found numerous applications, ranging from precise metrology (e.g. the SQUID) to novel computing paradigms (e.g. RSFQ logic or phase qubits).

The Josephson effect in fractal geometries has received only very limited attention in the literature so far.[19,20,24] In this paper, we fill this gap by considering a heterostructure made of a sandwich of conventional s-wave superconductors (S) and a normal material (N) with the Sierpiński fractal geometry. Note that in contrast to e.g. Ref. 19, we do not here consider fractal properties at the level of Josephson junction *arrays*,

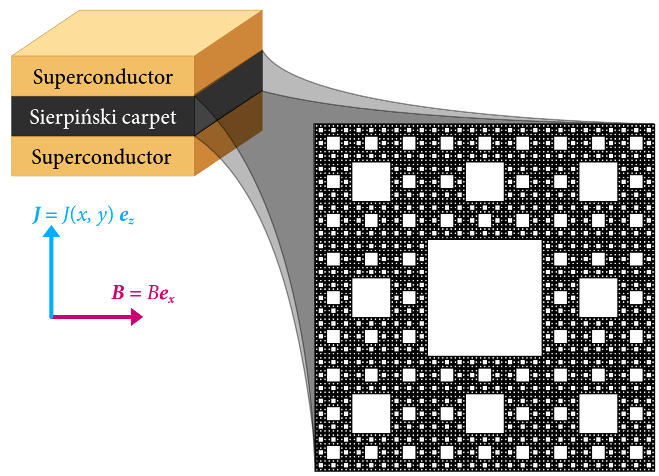

FIG. 1. Geometry of the S/N/S Josephson junction with the N layer exhibiting a fractal (self-similar) structure. The setup consists of two superconductors (yellow) connected by a normal metal (black) that has been patterned as a Sierpiński fractal by recursively creating insulating holes according to eq. (3). A homogeneous in-plane magnetic field $\boldsymbol{B} \sim \boldsymbol{e}_x$ is then applied to the Josephson junction, causing spatially varying screening currents $\boldsymbol{J} \sim \boldsymbol{e}_z$ to flow between the superconductors. Depending on the magnitude B of the applied magnetic field, the screening currents in different parts of the interlayer may either interfere constructively or destructively, causing a kind of interference pattern to appear in the current–field relation $I(B)$.

but rather a fractal structure within *one* junction. Moreover, while e.g. Refs. 20 and 24 consider interlayers with fractal characteristics that are naturally acquired during lithography, we here consider artificial fractal geometries that can exhibit much more dramatic phenomenology. In particular, we show that fractal geometry, here taken to be a Sierpiński carpet (fig. 1), has direct observable consequences on the Josephson effect. The form of the supercurrent-magnetic field relation in the process of the fractal generation, as we show, can be directly related to the self-similar fractal pattern of the normal metallic layer, as shown in fig. 2. Furthermore, the corresponding diffraction pattern, through its maxima, encodes the self-repeating fractal structure in the course of fractal generation (fig. 3), which implies that the corresponding magnetic length directly probes the shortest length scale in the given fractal generation. Our findings should motivate experimental pursuits to probe our theoretical predictions in the designer quantum materials.

We consider an S/N/S Josephson junction as illustrated in fig. 1.[22] We take the stack to be oriented along the z axis, and to have dimensions $W \times W$ in the xy plane. Each S layer is a conventional BCS superconductor,[25] and is assumed to be much longer than the magnetic penetration depth λ along the z direction. The N layer is a thin layer of a nominally normal metal, but has in our case been patterned as a Sierpiński carpet: It contains a fractal pattern of holes, where atoms have been removed from the otherwise normal metal in a self-similar and scale-invariant manner (see fig. 1). In an experiment, it is likely easier to deposit a thin layer of an electric insulator at the locations of the holes in our geometry, which would have the same effect as our missing lattice sites. Artificial fractal geometries in condensed matter systems—including Sierpiński fractals—have in recent years been experimentally realized.[6]

The Josephson effect between the two superconductors produces dissipationless currents that flow through the fractal layer whenever a phase difference is enforced. We assume that the Josephson penetration depth is much larger than the in-plane dimensions of the system, and hence any self-screening effects may be neglected, meaning that the currents flow solely in the z direction. The resulting current density therefore takes the form

$$\boldsymbol{J}(x, y) = J(x, y)\, \boldsymbol{e}_z = J_0 g(x, y) \sin[\varphi(x, y)]\, \boldsymbol{e}_z, \qquad (1)$$

where $\delta\varphi$ is the gauge-invariant phase difference between two vertically separated points deep inside each superconductor, and $g(x, y)$ is a form factor, indicating the shape of the fractal. To leading order, we have here assumed that the critical current density $J(x, y)$ is uniform and equal to J_0 at coordinates without a hole, whereas it drops to zero in the insulating holes. The critical current density is thus given as $J_c(x, y) = J_0 g(x, y)$. If we express the coordinates $x = ia$ and $y = ja$ in terms of a lattice constant a, we can then write

$$g(x, y) = S^N_{ij}, \qquad (2)$$

where S^N_{ij} are matrix elements of an N'th-order Sierpiński carpet. The Sierpiński carpet is a fractal structure that has the properties of self-similarity and scale invariance—at least down to the scale of individual unit cells—and is illustrated in fig. 1. Such a lattice may be constructed using the recursive algorithm

$$\boldsymbol{S}^N = \boldsymbol{S}^{N-1} \otimes \boldsymbol{S}^1, \qquad \boldsymbol{S}^1 = \begin{pmatrix} 1 & 1 & 1 \\ 1 & 0 & 1 \\ 1 & 1 & 1 \end{pmatrix}, \qquad \boldsymbol{S}^0 = 1, \qquad (3)$$

where $\otimes$ is the Kronecker matrix product. This implies that we can also write the N^{th} order Sierpiński carpet $\boldsymbol{S}^N = (\boldsymbol{S}^1)^{\otimes N}$ compactly as a Kronecker matrix power.

We now consider a magnetic field $\boldsymbol{B} = B\boldsymbol{e}_x$ applied in the thin-film plane of the fractal interlayer. This produces screening currents in the yz plane of the superconductors, within a distance on the order of their penetration depth λ away from the interface to the normal metal. These currents take the form of elongated loops that flow purely vertically through the thin normal metal, and give rise to a position-dependence in the gauge-invariant phase difference, $\phi = \phi_0 - \frac{2e}{\hbar} B d y$, where ϕ_0 is an externally enforced phase difference, and $d = l + 2\lambda$ is the effective thickness of the junction in the z direction, with l the

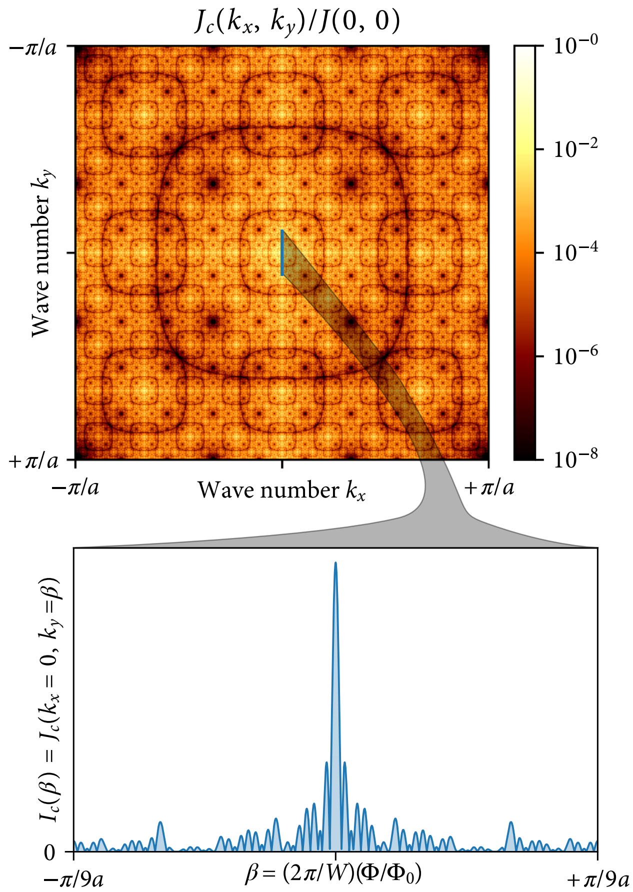

FIG. 2. Fourier transform $J_c(k_x, k_y)$ of the current distribution in a Sierpiński Josephson junction (upper panel). We here considered a 6th-order Sierpiński lattice as the interlayer. According to the Dynes–Fulton method, the net current $I(\beta)$ that arises for an applied magnetic field $B \sim \beta$ along the x axis is found from the Fourier-transformed current density along the y axis, as indicated by the blue line in the upper panel, with the result shown in the lower panel.

thickness of the normal metal. The result are spatially varying current contributions in the normal metal that can interfere constructively or destructively depending on the precise value of the magnetic field B. The total current flowing through the system at a given B is given as the surface integral over the cross section, which is quadratic with widths W,

$$I(B, \phi_0) = J_0 \int_{-W/2}^{W/2} \int_{-W/2}^{W/2} dxdy\; g(x, y) \sin\left[\phi_0 - \frac{2e}{\hbar} B dy\right], \tag{4}$$

As was first observed by Dynes and Fulton,[26] this expression is simply the imaginary part of the Fourier transform of the current density, which in our case becomes the Fourier transform of the fractal form factor, $g(k_x, k_y)$. Furthermore, since $g(x, y)$ has inversion symmetry, $g(k_x, k_y)$ is purely real. The critical current is thus found at $\phi = \pi/2$, and is given as

$$I_c(B) = |J_c(k_x = 0, k_y = \beta)| = J_0 \int d\boldsymbol{r}\; g(\boldsymbol{r}) e^{-i\beta y}, \tag{5}$$

with $\boldsymbol{r} = x\boldsymbol{e}_x + y\boldsymbol{e}_y$. Here, the magnetic field B is parametrized via $\beta = (2\pi/W)(\Phi/\Phi_0)$, where $\Phi = BWd$ is the net flux passing through the central parts of the Josephson junction, and $\Phi_0 = h/2e$ is the flux quantum.

Using the approach outlined above, the current–field relation $I_c(B)$ can be extracted as follows. First, an N^{th} order Sierpiński carpet is constructed recursively using eq. (3). This is subsequently employed to find $J_c(x, y)$ according to eqs. (1) and (2), which can then be run through a 2D Fast Fourier Transform (FFT) algorithm to obtain $J_c(k_x, k_y)$. Finally, we can then simply extract the critical current along a line in the 2D plane, as determined by the direction of the applied field and the chosen gauge. This procedure, and the resulting $I_c(B)$, are shown in fig. 2 for a junction with a 6th-order Sierpiński interlayer. Unsurprisingly, the Fourier transform of a fractal contains self-similar features also, and ends up having structures on all length scales from π/W to π/a. The resulting field dependence has a very different structure from the well-known Fraunhofer and SQUID patterns that arise in comparable non-fractal junctions.

We can arrive at this result by purely analytical means. This can be done by treating current as a parallel coupling of the current passing through each of the constituent elements of a generation of the Sierpiński carpet. To illustrate this we consider, for instance, the first generation, as is obtained from fig. 1 by retaining only the largest hole in the center. In that case, the total current may be split into three parts, two of which form rectangular junctions with dimensions $W \times W/3$, and one part which has the form of a SQUID formed by two junctions with dimensions $W/3 \times W/3$ and an equally sized hole in between. The rectangular contributions provide a current in a Fraunhofer pattern, $J_0 \frac{W^2}{3} \operatorname{sinc}(\pi N_\Phi)$, whereas the SQUID contribution gives a current $2J_0 \left(\frac{W}{3}\right)^2 \operatorname{sinc}\left(\frac{\pi N_\Phi}{3}\right) \cos\left(\frac{2\pi N_\Phi}{3}\right)$. Here, $N_\Phi = BdW/\Phi_0$ is the number of flux quanta passing through the system, and $\operatorname{sinc}(x) = \sin(x)/x$. Adding up each contribution gives the critical current for the first-generation Sierpiński carpet

$$I_c^{(1)}(B) = \frac{J_0 A_F^{(1)}}{4} \left| \operatorname{sinc}\left(\frac{\pi N_\Phi}{3}\right) \left[1 + 3\cos\frac{2\pi N_\Phi}{3}\right] \right|,$$

where $A_F^{(N)} = \left(\frac{8}{9}\right)^n W^2$ is the surface area of the fractal at generation n. An expression for arbitrary generation N can be obtained by repeating this process recursively, replacing each uniform sub-square with the shape of the previous generation. This leads to

$$I_c^{(N)}(B) = \frac{J_0 A_F^{(N)}}{4^N} \left| \operatorname{sinc}\left(\frac{\pi N_\Phi}{3^N}\right) \prod_{n=1}^{N} \left[1 + 3\cos\left(\frac{2\pi N_\Phi}{3^n}\right)\right] \right|, \tag{6}$$

The 0th-order Sierpiński carpet is equivalent to a uniform square lattice, and indeed we regain the conventional Fraunhofer pattern for $N = 0$ when no terms appear in the right-hand product, $I_c^{(0)}(B) = J_0 W^2 \operatorname{sinc}(\pi N_\Phi)$. In the opposite limit $N \to \infty$ of a high-order Sierpiński carpet, the prefactor approaches $\operatorname{sinc}(0) = 1$. The current–field relation then reduces to a product of similar factors $1 + 3\cos(\beta W_n)$ arising from the Sierpiński pattern on different scales $W_n = W/3^n$. This result shows clearly that $I_c(B)$ exhibits self-similarity across different length scales, which arises from the fractal geometry of the

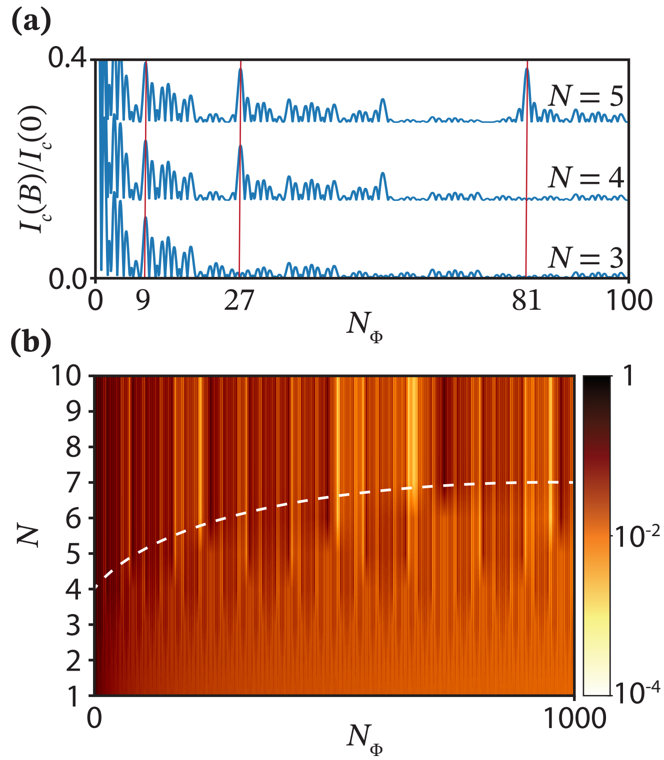

FIG. 3. The critical current I_c as a function of magnetic field, $N_\Phi = BdW/\Phi_0$, for various generations N of the Sierpiński carpet. (a) Line plots for $N \in \{3, 4, 5\}$, shifted vertically for clarity. The vertical lines indicate the location of new peaks introduced by an increase in N. (b) A surface plot of $I_c(B)$ for a wider range of values of N and N_Φ. The dashed line is a guide for the eye, showing approximately where $I_c(B)$ becomes independent of N.

Josephson junction interlayer. This self-similarity can be seen in the 2D Fourier transform in fig. 2, where it manifests as superimposed lattices of $3^n \times 3^n$ squares.

The presence of multiple length scales has additional nontrivial observable consequences as, for instance, the sensitivity of the diffraction pattern on the order of fractal generation. In fig. 3(a) the diffraction pattern is shown for a selection of fractal generations, $N \in \{3, 4, 5\}$. It can be seen that each new generation introduces new features in the diffraction pattern which were not present in the previous one. These features appear in limited ranges of N_Φ, and are characterized by a single peak of constant height, the location of which is indicated by the vertical lines in fig. 3(a). Indeed, for a fixed N, we observe that whenever $N_\Phi = 3^q$ for an integer q, the square brackets in eq. (6) become constant and maximal for all $n \le q$. For $q < N$, $I_c^{(N)}$ increases with q, whereas for $q \ge N$ it vanishes. The result is a local maximum at $q = N - 1$, at which point the critical current becomes $I_c^{(N)} = 3\sqrt{3} J_0 A_F^{(N)}/16\pi$. The peak occurring at $N_\Phi = 3^{N-1}$ is a manifestation of the fact that the magnetic length scale becomes small enough to resolve the lowest length scales of the fractal. Alternatively, one may say that when fractal generation is increased from N to $N + 1$, the smallest length scale is reduced by a factor of 3. Hence, a flux density corresponding to the rescaled magnetic field, $3B$, in the latter (generation $N + 1$), produces a similar response as B in the former case (generation N). Another interesting and related feature is that the critical current for any N_Φ eventually becomes independent of N. This is demonstrated in fig. 3(b), which shows a surface plot of the critical current as a function of N and N_Φ. The dashed line indicates approximately where this saturation occurs. For $N = 7$, the diffraction pattern remains constant at least for $N_\Phi \le 1000$. This behavior is once again a result of the phenomenon that as N increases, smaller and smaller length scales are introduced, which eventually become smaller than the magnetic length scale. Their features cannot be resolved by the applied flux, and so the system remains uninfluenced.

Here, we have focused on the specific case where the magnetic field $\boldsymbol{B} \sim B\boldsymbol{e}_x$ is applied along the x axis. Note however that a similar Dynes–Fulton analysis is applicable for a magnetic field $\boldsymbol{B}(\theta) = B(\cos\theta\, \boldsymbol{e}_x + \sin\theta\, \boldsymbol{e}_y)$ oriented along any direction in the $x - y$ plane, where each such direction would provide a slightly different current–field relation $I_c(B \,|\, \theta)$. In principle, one could in an experiment use the $I_c(B \,|\, \theta)$ curves obtained for different field directions θ to reconstruct the 2D Fourier transform $J_c(k_x, k_y)$ of the current density, and thus to obtain the exact current distribution $J_c(x, y)$ in the interlayer. Such an approach might be particularly interesting in Josephson junctions where the interlayer might not be an artificially constructed fractal as considered here, but rather a naturally occurring fractal or quasicrystal. In that case, this kind of Dynes–Fulton analysis might provide a way to validate and elucidate the non-crystalline, fractal or quasicrystalline, structure of the interlayer.

In this paper, we have considered a fractal Josephson junction composed of two superconductors separated by a Sierpiński-patterned normal metal. We have analytically calculated the current–field relation $I_c(B)$ that arises in such junctions, and shown that this experimental signature retains a crucial property of fractals: self-similarity across length scales. In particular, the obtained diffraction pattern is directly related to the self-similar fractal geometry probed through the magnetic length. Our results should be consequential for experiments, particularly in the designer quantum materials, where the realization of the normal fractal metallic layer should be feasible.

M.A. was supported by the Research Council of Norway through its Centres of Excellence funding scheme Grant No. 262633 "QuSpin". V.J. acknowledges the support of the Swedish Research Council Grant No. VR 2019-04735 and Fondecyt (Chile) Grant No. 1230933.

Data Availability

Data sharing is not applicable to this article as no new data were created or analyzed in this study.

[1] B. B. Mandelbrot, *The fractal geometry of Nature* (W.H. Freeman and Co., 1982).

[2] D. R. Hofstadter, "Energy levels and wave functions of bloch electrons in rational and irrational magnetic fields," Phys. Rev. B **14**, 2239–2249 (1976).

[3] C. M. Soukoulis and E. N. Economou, "Fractal character of eigenstates in disordered systems," Physical Review Letters **52**, 565–568 (1984).

[4] M. Schreiber and H. Grussbach, "Multifractal wave functions at the Anderson transition," Physical Review Letters **67**, 607–610 (1991).

[5] J. Shang, Y. Wang, M. Chen, J. Dai, X. Zhou, J. Kuttner, G. Hilt, X. Shao, J. M. Gottfried, and K. Wu, "Assembling molecular Sierpiński triangle fractals," Nature Chemistry **7**, 389–393 (2015).

[6] S. N. Kempkes, M. R. Slot, S. E. Freeney, S. J. M. Zevenhuizen, D. Vanmaekelbergh, I. Swart, and C. M. Smith, "Design and characterization of electrons in a fractal geometry," Nature Physics **15**, 127–131 (2019).

[7] M. Brzezińska, A. M. Cook, and T. Neupert, "Topology in the Sierpiński–Hofstadter problem," Physical Review B **98**, 205116 (2018).

[8] S. Pai and A. Prem, "Topological states on fractal lattices," Physical Review B **100**, 155135 (2019).

[9] A. A. Iliasov, M. I. Katsnelson, and S. Yuan, "Hall conductivity of a Sierpiński carpet," Physical Review B **101**, 045413 (2020).

[10] S. Manna, B. Pal, W. Wang, and A. E. B. Nielsen, "Anyons and fractional quantum Hall effect in fractal dimensions," Physical Review Research **2**, 023401 (2020).

[11] M. Fremling, M. van Hooft, C. M. Smith, and L. Fritz, "Existence of robust edge currents in sierpiński fractals," Physical Review Research **2**, 013044 (2020).

[12] Z. Yang, E. Lustig, Y. Lumer, and M. Segev, "Photonic floquet topological insulators in a fractal lattice," Light: Science & Applications **9**, 128 (2020).

[13] S. Manna, C. W. Duncan, C. A. Weidner, J. F. Sherson, and A. E. B. Nielsen, "Anyon braiding on a fractal lattice with a local Hamiltonian," Physical Review A **105**, L021302 (2022).

[14] S. Manna, S. Nandy, and B. Roy, "Higher-order topological phases on fractal lattices," Physical Review B **105**, L201301 (2022).

[15] M. N. Ivaki, I. Sahlberg, K. Pöyhönen, and T. Ojanen, "Topological random fractals," Communications Physics **5**, 327 (2022).

[16] S. Manna and B. Roy, "Inner skin effects on non-Hermitian topological fractals," Communications Physics **6**, 10 (2023).

[17] M. Hori, T. Sugimoto, T. Tohyama, and K. Tanaka, "Self-consistent study of topological superconductivity in two-dimensional quasicrystals," (2024), arXiv:2401.06355.

[18] A. A. Iliasov, M. I. Katsnelson, and A. A. Bagrov, "Strong enhancement of superconductivity on finitely ramified fractal lattices," (2024), arXiv:2310.11497.

[19] R. Meyer, S. E. Korshunov, C. Leemann, and P. Martinoli, "Dimensional crossover and hidden incommensurability in Josephson junction arrays of periodically repeated Sierpiński gaskets," Physical Review B **66**, 104503 (2002).

[20] S. T. Kingni, G. F. Kuiate, V. K. Tamba, A. V. Monwanou, and J. B. C. Orou, "Analysis of a fractal Josephson junction with unharmonic current–phase relation," Journal of Superconductivity and Novel Magnetism **32**, 2295–2301 (2019).

[21] S. Manna, S. K. Das, and B. Roy, "Noncrystalline topological superconductors," (2022), arXiv:2207.02203.
[22] B. Josephson, "Possible new effects in superconductive tunnelling," Physics Letters **1**, 251–253 (1962).
[23] A. A. Golubov, M. Y. Kupriyanov, and E. Il'ichev, "The current–phase relation in Josephson junctions," Reviews of Modern Physics **76**, 411–469 (2004).
[24] S. P. Kruchinin, V. F. Klepikov, V. E. Novikov, and D. S. Kruchinin, "Nonlinear current oscillations in the fractal Josephson junction," Materials Science Poland **23**, 1009 (2005).
[25] J. Bardeen, L. N. Cooper, and J. R. Schrieffer, "Theory of superconductivity," Physical Review **108**, 1175–1204 (1957).
[26] R. C. Dynes and T. A. Fulton, "Supercurrent density distribution in Josephson junctions," Physical Review B **3**, 3015–3023 (1971).